Materials Science-Poland, 33(4), 2015, pp. 867-878
http://www.materialsscience.pwr.wroc.pl/
DOI: 10.1515/msp-2015-0106

DE GRUYTER OPEN

Investigations of structural, elastic, electronic and thermodynamic properties of lutetium filled skutterudite $LuFe_4P_{12}$ under pressure effect: FP-LMTO method

KELTOUMA BOUDIA[1], MOHAMMED AMERI[1]*, Y. AL-DOURI[2], IBRAHIM AMERI[3], H. BOUAFIA[4]

[1]Laboratory of Physical Chemistry of Advanced Materials, University of Djillali Liabes, BP 89, Sidi-Bel-Abbes 22000, Algeria

[2]Institute of Nano Electronic Engineering, University Malaysia Perlis, 01000 Kangar, Perlis, Malaysia

[3]Djillali Liabes University, Faculty of Exact Sciences, Department of Physics, PO Box 089, Sidi Bel Abbes, 22000, Algeria

[4]Electron Microscopy Laboratory (USTO) Oran, Algeria

Structural, elastic, electronic and thermodynamic properties of ternary cubic filled skutterudite compound were calculated. We have computed the elastic modulus and its pressure dependence. From the elastic parameter behavior, it is inferred that this compound is elastically stable and ductile in nature. Through the quasi-harmonic Debye model, in which phononic effects are considered, the effect of pressure P (0 to 50 GPa) and temperature T (0 to 3000 °C) on the lattice constant, elastic parameters, bulk modulus B, heat capacity, thermal expansion coefficient α, internal energy U, entropy S, Debye temperature θ_D, Helmholtz free energy A, and Gibbs free energy G are investigated.

Keywords: *FP-LMTO; structural properties; elastic properties; electronic properties; thermodynamic properties.*

1. Introduction

Skutterudite compounds named after Skutterud region in Norway have the chemical formula M X_3, where M is a metal and X a pnictogen [1]. The filled skutterudites have the formula M T_4 X_{12}, where M can be an alkaline earth, lanthanide or actinide ion, T is Fe, Ru, or Os, and X is P, As, or Sb and crystallize in the cubic skutterudite LaFe4P12 structure (space group Im3) [2]. The filled skutterudites attracted attention because of their large thermoelectric potential as well as of the rich variety of observed ground-state properties [3]. Many of the extraordinary properties of these compounds are associated with M ion that occupies the atomic "cage" in the binary ("unfilled") $CoAs_3$ type skutterudite structure. Investigation of the filled skutterudite compounds remains an active field, because of their interesting ground state behaviors which include unconventional super-conductivity [4, 5], magnetism [6, 7]. heavy fermions [8] and non-Fermi liquid behavior [9]. We have prepared many filled skutterudites with lighter lanthanide at high temperatures and high pressures [10–12]. The physical properties of the filled skutterudites depend on M atom hybridization between f-electron states of the M atom with the conduction electron states. The structural properties of $LuFe_4P_{12}$ filled skutterudites are determined using the neutron diffraction technique [13]. Besides, one of the most important properties is characterized by X-ray diffraction using CuKα radiation and silicon as a standard at ambient pressure [14].

The purpose of this work is to clarify the physical properties of filled skutterudite $LuFe_4P_{12}$ and provide a comparative study of structural, electronic, elastic and thermodynamic properties, using the first principle calculations and following full-potential linear muffin-tin orbital (FP-LMTO) method within local density approximation (LDA)

*E-mail: lttnsameri@yahoo.fr

using exchange-correlation (XC) potential. The organization of this paper is as follows: we describe the FP-LMTO computational details in Section 2, and in Section 3, the results and discussion of structural, electronic, elastic and thermodynamic properties are presented. Finally, conclusions are given in Section 4.

Table 1. The number of plane wave (NPW), energy cut-off (in Ry) and the muffin-tin radius (MTS) (in a.u.), used in our calculations for $LuFe_4P_{12}$.

	$LuFe_4P_{12}$		
NPW			
LDA	34412		
LSDA	34412		
$E_{cut\text{-}off}$ (Ry)			
LDA	124.1905		
LSDA	130.1176		
Atom			
MTS (a.u.)	Lu	Fe	p
LDA	3.384	2.055	2.055
LSDA	3.370	2.030	2.112

2. Computational method

It is of interest to find out the most convenient method to know deeply the studied compound properties and its behaviour. Therefore, our attention is centred on the atomic structure and dimensions studied according to the methods using the full potential linear muffin-tin orbital (FP-LMTO) method augmented by a plane-wave (PLW) basis [15, 16] and implemented in the Lmtart computer code [17]. In this method, the space is divided into interstitial regions (IR) and non-overlapping (MT) spheres centered on the atomic sites. In the IR regions, the Fourier series represents the basic functions. Inside MT spheres, the basic set is treated as a linear combination of radial functions times spherical harmonics. In order to achieve a satisfactory degree of convergence of energy eigenvalues, the wave functions in the interstitial regions are expanded into plane waves with an energy cut-off equal to 124 Ry and the number of plane wave equal to 34412. The values of muffin-tin sphere radius (MTS) are taken to be 338.4, 205.5 and 205.5 (pm) for Lu, Fe and P, respectively. The valence wave functions inside the spheres are expanded up to $l_{max} = 6$. The exchange-correlation (XC) effects are treated within a local density approximation (LDA) [18, 19]. The K integrations over the Brillouin zone (BZ) are performed up to (6 6 6) grid (yielding 18 k-points in the irreducible Brillouin zone (IBZ) using the tetrahedron method [20]. The values of the spherical radius (MTS), energy cut-off and the number of plane waves (PLWS) found in the previous calculations are given in Table 1.

3. Results and discussions

3.1. Structural properties

The $LuFe_4P_{12}$ compound crystallizes in the cubic space group Im3 (#204). The Lu, Fe and P atoms are located at (0 0 0), (1/4 1/4 1/4) and (0 y z) Wyckoff positions, respectively. The crystal structure of $LuFe_4P_{12}$ is shown in Fig. 1. The skutterudite structure is characterized by two non-equivalent atomic positions y and z, which are not fixed by symmetry. The y and z positions have been optimized by minimizing the total energy with keeping the volume fixed at the experimentally observed value to compare the calculated values with other theoretical and experimental data of the ternary skutterudites $LuFe_4P_{12}$ as given in Table 2. The optimized values of y and z are used to calculate the total energy at different unit-cell volumes. Fig. 2 shows the calculated total energies as a function of the unit cell volume for $LuFe_4P_{12}$ local density approximation (LDA). The curve of the total energy versus unit cell volume is fitted to Murnaghan's equation of state (EOS) [21] to determine the ground state properties, such as the equilibrium lattice constant a_0, the bulk modulus B_0 and its pressure derivative B'. The calculated values of y, z, a_0, B_0 and B' for the studied compound are summarized in Table 2.

3.2. Electronic properties

3.2.1. Band structure

The band structure of the filled skutterudites under study, which was calculated as shown in

Table 2. Lattice constant a_0 (in Å), atomic positions y and z for P atom, bulk modulus B (in GPa), its pressure derivative B′ and the minimum energy at the equilibrium E_0 (in Ry) for $LuFe_4P_{12}$. Experimental data are quoted for comparison.

$LuFe_4P_{12}$	a_0	Y	Z	B	$B^{'}$	E_0
Present	7.6747^{LDA}	0.3503^{LDA}	0.1491^{LDA}	193.399^{LDA}	3.4502^{LDA}	−47493.9661
	7.6527^{LSDA}		209.6995^{LSDA}	3.3027^{LSDA}	−47493.96166	
Exp.						
(UFe_4P_{12})[36]	7.7729					
(UFe_4P_{12})[13]	7.2228	0.1494	0.3506			
Other. calc.						
($LuFe_4P_{12}$)[42]	7.7771 (3)					
($PrFe_4P_{12}$)[34]	7.6776	0.3525	0.151	186.7916	3.6965	−236821.45838
(UFe_4P_{12})[35]	7.6510	0.3503	0.1491	199.227	3.585	
(La Fe_4P_{12})[37]	7.8316	0.3539	0.1504			
(Ce Fe_4P_{12})[38]	7.7920	0.3522	0.1501			

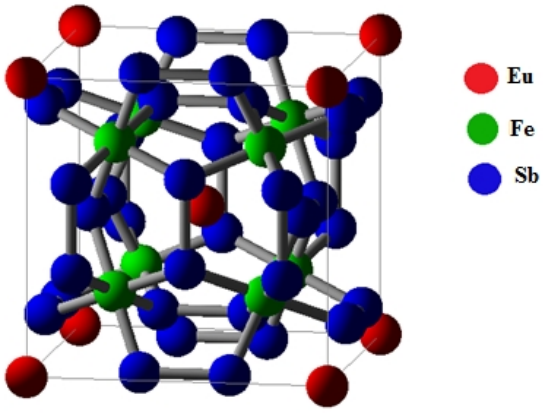

Fig. 1. The model of filled skutterudite.

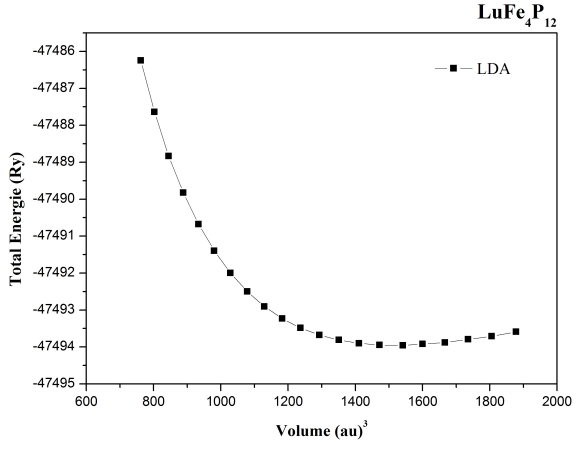

Fig. 2. The variation of total energy with unit cell volume for $LuFe_4P_{12}$.

Fig. 3, yields an indication of the valence band (VB) and conduction band (CB); the Fermi level (E_F) is indicated by a horizontal dotted line. The band structure for $LuFe_4P_{12}$ is shown in Fig. 3 for spin-up and spin-down electrons. The band structure of $LuFe_4P_{12}$ appears above the Fermi level at Γ point for both spin up and spin down electrons.The region is mainly formed by the valence 4f-electron states of Lu with a very small contribution of the 3d states for the channel spin (Fig. 3). A strong peak due to Lu-4f states is 0.168 eV in the spin-up channel (Fig. 3a). The conduction region is mainly due to Lu-4f states that give rise to a sharp peak at 0.150 eV in the spin down link channel (Fig. 3b), To understand the electronic properties of $LuFe_4P_{12}$, the calculation of electronic band structure along the direction of the vertices of symmetry in the Brilllouin zone is shown in Fig. 3 for the two spin channels. From the band structure plots, we notice that there is an overlap between the conduction and valence bands for both spin up and spin down, which means that this compound has metallic character.

3.3. Elastic properties

The elastic properties provide information about capability of materials deformation under applied external forces. Therefore, the stability, stiffness and structural phase of materials are

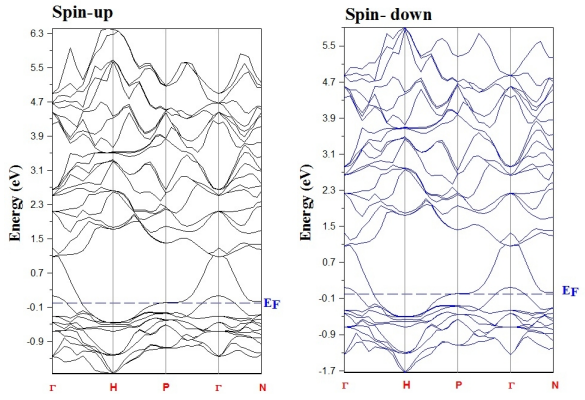

Fig. 3. Band structure obtained by means of LSDA.

changed. For our studied compound, which has a cubic crystal structure, there are only three different symmetry elements: C_{11}, C_{12} and C_{44} which in turn represent three coupled equalities: $C_{11} = C_{22} = C_{33}$, $C_{12} = C_{23} = C_{31}$ and $C_{44} = C_{55} = C_{66}$. The elastic constants C_{ij} are obtained by calculating the total energy as a function of volume conserving strains using the Mehl method [22], which has been applied with successful results in previous works on some skutterudite compounds [23–26]. By imposing the conservation of volume of the sample under pressure effect, the first equation involves the elastic moduli $(C_{11} - C_{12})$ which are related to the bulk modulus B by the following expression:

$$B = (C_{11} + 2C_{12})/3 \tag{1}$$

The second one involves applying volume conserving orthorhombic strain tensor:

$$\bar{\varepsilon} = \begin{bmatrix} \delta & 0 & 0 \\ 0 & \delta & 0 \\ 0 & 0 & \frac{1}{(1+\delta^2)} - 1 \end{bmatrix} \tag{2}$$

The total energy is influenced by the application of this strain and is expressed as:

$$E(\delta) = E(-\delta) = E(0) + 6(C_{11} - C_{12})V_0\delta^2 + O(\delta^4) \tag{3}$$

For identification of C_{44}, we used a monoclinic strain conserving volume defined as:

$$\bar{\varepsilon} = \begin{bmatrix} 1 & \frac{\delta}{2} & 0 \\ \frac{\delta}{2} & 1 & 0 \\ 0 & 0 & \frac{4}{(4-\delta^2)} \end{bmatrix} \tag{4}$$

which changes the total energy into:

$$E(\delta) = E(-\delta) = E(0) + \frac{1}{2}C_{44}V_0\delta^2 + O(\delta^3) \tag{5}$$

The corresponding energy results then from the stress applied to the orthorhombic (a) and monoclinic (b) phase of the studied compound, that is $LuFe_4P_{12}$. Combining equation 1 and equation 4, one can easily determine the two elastic constants C_{11} and C_{12}, while the third elastic constant C_{44} is derived by equation 5. From the elastic constants we obtain the anisotropy parameter A (for an isotropic crystal, A is equal to 1, while another value greater or less than 1 means that it is an anisotropic crystal) which deviates much from unity, that is characteristic of profound anisotropy. Other important mechanical quantities, such as the shear modulus G, Young's modulus E and Poisson's ratio ν are often measured for polycrystalline materials when investigating their hardness, and calculated in terms of the computed elastic constants C_{ij} using the following relations [22–24]:

$$A = \frac{2C_{44}}{C_{11} - C_{12}} \tag{6}$$

$$\nu = \frac{3B - E}{6B} \tag{7}$$

$$E = \frac{9BG}{3B + G} \tag{8}$$

$$G = \frac{C_{11} - C_{12} + 3C_{44}}{5} \tag{9}$$

where B is bulk modulus given by equation 1. From these results, we find that the stability criteria [25, 26]; $C_{11} - C_{12} > 0$, $C_{11} > 0$, $C_{44} > 0$,

$(C_{11}+2C_{12}) > 0$ and $C_{12} < B < C_{11}$, are satisfied for the studied skutterudites, and, therefore, it is elastically stable.

The calculated elastic constants C_{ij}, bulk modulus B, shear modulus G, Young's modulus E, Poisson's ratio ν, the anisotropic parameter A and B/G rations of $LuFe_4P_{12}$ at different pressures using LDA calculation are summarized in Table 3. We have presented our calculated values of the elastic constants C_{11}, C_{12}, C_{44}, bulk modulus B, shear modulus G and Young's modulus E. The variation of the relative energy with respect to the square of tetragonal and monoclinic strains, illustrated in Fig. 4, has been used for determining $C_{11} - C_{12}$ and C_{44} in the pressure range from 0 GPa to 50 GPa with steps of 10 GPa. It is seen that the calculated total energy varies linearly with the applied stress. The calculated slopes are found to be equal to 53.5 and 21.1 Ry for the orthorhombic and monoclinic constraints, respectively, at zero pressure. The variations of C_{11}, C_{12}, C_{44} and the bulk modulus B, shear modulus G and Young's modulus E under pressure effects are presented in Fig. 5. Our results show that all elastic constants increase as the pressure increases, C_{11} is more sensitive to the change in pressure compared to the other elastic constants C_{12} and C_{44} which are less sensitive to the change of pressure. In Table 3, the value of bulk modulus B calculated by expression 1 at $P = 0$ GPa is documented. It is noted that the calculated value is nearly the same as that obtained from fitted Murnaghan's equation of state.

A typical Poisson's ratio value of 0.25 suggests a high ionic contribution in intra-atomic bonding for this compound. For $LuFe_4P_{12}$ skutterudite alloy, it varies between 0.2884 and 0.3416 (Table 3) for various pressures indicating that this compound is ionic. The Young's modulus of materials is defined as the ratio of linear stress and linear strain, which gives information about the stiffness. The obtained values of the Young's modulus of our compound are higher than 90 GPa; thus, this material will show large stiffness. One of the most important properties of crystalline solids is the elastic anisotropy ratio represented by equation 6. This property has an important implication in engineering science since it is highly correlated with the possibility to introduce microcracks in materials [27]. Essentially, all known crystals are elastically anisotropic. For isotropic crystals A equals to 1.0, while any value smaller or larger than 1.0 indicates anisotropy. The magnitude of deviation from 1.0 is a measure of degree of elastic anisotropy possessed by the crystal. In our case, the anisotropic A values vary from 1.3752 to 2.3184 at various pressures, indicating that the material is characterized by a profound anisotropy. According to the Pugh's empirical formula [28], the critical value which separates ductile and brittle materials is around 1.75. If $B/G > 1.75$, the material behaves in a ductile manner; otherwise the material behaves in a brittle manner. In our case, the ratio of B/G values varies from 2.0949 to 2.8224 at various pressures, revealing the slight ductility of this compound.

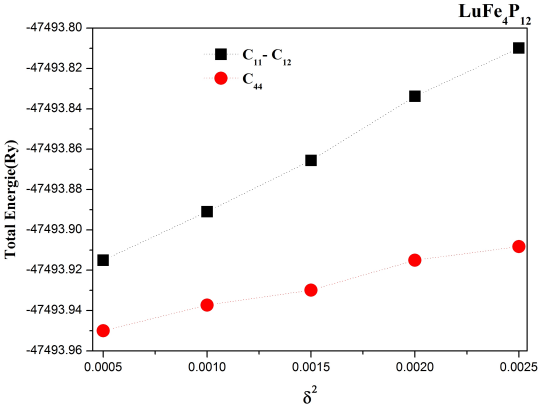

Fig. 4. Energy as a function of square orthorhombic and monoclinic strain used to determine $C_{11} - C_{12}$ and C_{44}.

3.4. Debye temperature

The Debye temperature θ_D is one of the most important parameters that determines the thermal characteristics of materials. It is used to distinguish between the high and low temperature regions in solids. One of the standard methods to calculate the Debye temperature θ_D is from the elastic constants data using the following expression [29]:

$$\theta_D = \frac{h}{k_B}\left[\frac{3n}{4\pi V_a}\right]^{\frac{1}{3}} \nu_m \qquad (10)$$

Table 3. Calculated elastic constants C_{11}, C_{12}, C_{44} (in GPa), bulk modulus (in GPa), Young and shear modulus E in GPa, G (in GPa), Poisson's ratio ν, and the anisotropic parameter A for $LuFe_4P_{12}$.

P	C_{11}	C_{12}	C_{44}	B	G	E	ν	A	B/G
0	278.9173	149.741	115.2731	192.80	94.99906	244.791512	0.2884	2,3184	2.02949
($PrFe_4P_{12}$)[40]	437.557	1.408	156.288	186.791	169.00246	389.53	0.931	0.152	1.10
(UFe_4P_{12})[41]	524.11	36.787	386.83	199.227	329.56	637.83	1.59	−0.003	0.60
+10	333.5667	173.986	116.241	227,18	101.6607	265.3951	0.3053	1.4568	2.2346
+20	375.7871	204.386	124.793	261,52	109.1559	287.4720	0.3168	1.4562	2.3958
+30	416.978	235.347	137.9287	295,89	119.0835	314.9932	0.3226	1.5188	2.4847
+40	458.5137	266.178	132.2462	330,29	117.8149	315.8857	0.3406	1.3752	2.8035
+50	499.9092	297.053	147.7487	364,71	129.2205	346.7134	0.3416	1.4541	2.8224

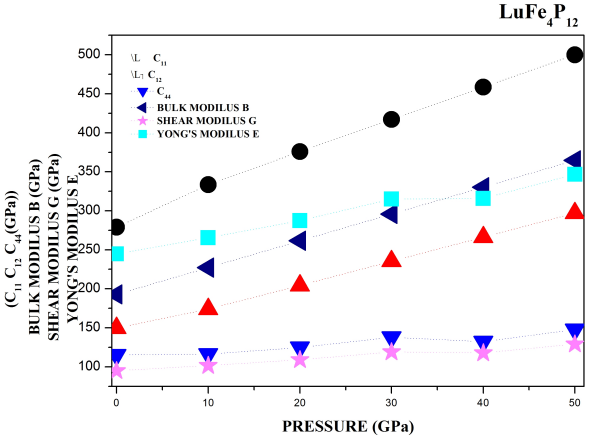

Fig. 5. Total elastic constants C_{11}, C_{12}, C_{44} (in GPa), bulk modulus (in GPa), shear modulus G (in GPa) and Yong's modulus E (in GPa) as a function of pressure.

where h is Planck's constant, k_B is the Boltzmann constant, V_a is the atomic volume and n is the number of atoms per unit volume. The average sound velocity ν_m in the polycrystalline material is given by Voigt [30]:

$$\nu_m = \left[\frac{1}{3}\left(\frac{2}{\nu_t^3} + \frac{1}{\nu_l^3}\right)\right]^{-\frac{1}{3}} \tag{11}$$

where ν_l and ν_t are the longitudinal and transverse sound velocities in an anisotropic material, which can be obtained using the shear modulus G and the bulk modulus B from Navier's equations [31]:

$$\nu_l = \left(\frac{3B+4G}{3\rho}\right)^{\frac{1}{2}} \tag{12}$$

$$\nu_t = \left(\frac{G}{\rho}\right)^{\frac{1}{2}} \tag{13}$$

The calculated sound velocities and Debye temperature as well as the density at different pressures using LDA approximation are given in Table 4. The results indicate that the values of ν_l, ν_t, ν_m and θ_D increase as the pressure increases. To the best of our knowledge there are no experimental and other theoretical data available in the literature for comparison, so we consider the present results as a prediction study, carried out for the first time, which still awaits an experimental confirmation. Fig. 6. shows the variation of the longitudinal, transverse and medium speed as functions of pressure. It is clear that the longitudinal speed increases linearly with increasing pressure in a very steep slope of about 45.03 in comparison to the small slope for the average and transverse velocities are of the order of 13.33 and 15.64, respectively.

3.5. Thermodynamic properties

To investigate the thermal properties of $LuFe_4P_{12}$ compound at high temperature and high pressure, we have applied the quasi-harmonic Debye model as implemented in the Gibbs program [32]. The non-equilibrium Gibbs function $G^*(V, P, T)$ takes the form:

$$G^*(V,P,T) = E(V) + PV + A_{vib}[\theta(V);T] \tag{14}$$

where E(V) is the total energy for $LuFe_4P_{12}$, PV is the hydrostatic pressure condition, θ(V) is the

Table 4. Longitudinal, transverse and average sound velocities (ν_l, ν_t, ν_m), (in ms^{-1}), and Debye temperature (θ_D, in K) calculated with LDA at different pressures for $LuFe_4P_{12}$.

P (GPa)	ν_l (ms^{-1})	ν_t (ms^{-1})	ν_m (ms^{-1})	θ_D (K)
0	7665.355	4180.036	4662.204	624.7651
10	8167.05	4324.112	4833.193	675.963
20	8652.573	4480.683	5015.611	723.5
30	9144.628	4680.001	5242.667	762.3
40	9467.877	4655.000	5227.099	800.3
50	9938.230	4875.127	5474.970	836.25

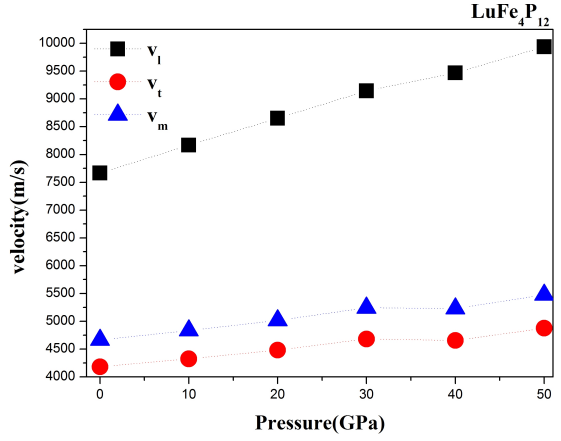

Fig. 6. Pressure dependence of the longitudinal, transverse and average sound velocity (v_l, v_t and v_m in m/s) for $LuFe_4P_{12}$.

Debye temperature, and A_{vib} is the Helmholtz free energy, which can be written as [32, 33]:

$$A_{vib}(\theta_D, T) = nK_BT\left[\frac{9\theta_D}{8T} + 3\ln(1-e^{-\theta_D/T}) - D\left(\frac{\theta_D}{T}\right)\right] \quad (15)$$

where n is the number of atoms per formula unit, D (θ/T) is the Debye integral. The Debye temperature θ is given as [33]:

$$\theta_D = \frac{\hbar}{K_B}(6\pi^2 nV^{\frac{1}{2}})^{\frac{1}{3}} f(\sigma)\sqrt{\frac{B_S}{M}} \quad (16)$$

where M is the molecular mass per unit cell and B_S is the adiabatic bulk modulus, which is approximately given by static compressibility [32]:

$$B_s \approx B(V) = V\frac{d^2E(V)}{dV^2} \quad (17)$$

f(σ) is given in the literature [34, 35]:

$$f(\sigma) = \left\{3\left[2\left(\frac{2+\sigma}{3-2\sigma}\right)^{\frac{3}{2}} + \left(\frac{1+\sigma}{3-\sigma}\right)^{\frac{3}{2}}\right]^{-1}\right\}^{\frac{1}{3}} \quad (18)$$

where σ is Poisson ratio. Therefore, the non-equilibrium Gibbs function G*(V, P, T) as a function of (V, P, T) can be minimized with respect to volume V as:

$$\left[\frac{\delta G^*(V,P,T)}{\delta V}\right]_{P,T} = 0 \quad (19)$$

The thermal equation of state (EOS) V(P, T) can be obtained by solving equation 20. The isothermal bulk modulus B_T is given by Blanco et al. [32]:

$$B_T(P,T) = V\left(\frac{\delta^2 G^*(V,P,T)}{\delta^2 V}\right)_{P,T} \quad (20)$$

The thermodynamic quantities, e.g. heat capacities C_V at stable volume and C_P at stable pressure, entropy S, and internal energies have been calculated by applying the following relations [32]:

$$C_V = 3nK_B\left[4D\left(\frac{\theta_D}{T}\right) - \frac{\left(\frac{3\theta_D}{T}\right)}{e^{\theta_D/T}-1}\right] \quad (21)$$

$$C_P = C_v(1+\alpha\gamma T) \quad (22)$$

$$S = nK[4D(\theta/T) - 3\ln(1-e^{-\theta/T})] \quad (23)$$

$$U = nkT\left[\frac{9}{8}\frac{\theta}{T} + 3D\left(\frac{\theta}{T}\right)\right] \quad (24)$$

where α is the thermal expansion coefficient and γ is the Grüneissen parameter which is given by Blanco et al. [32]:

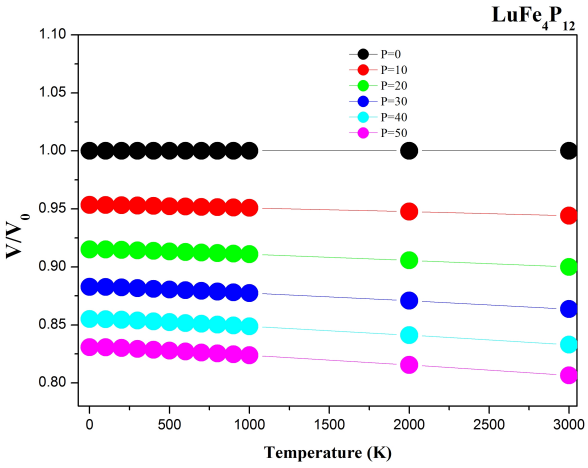

Fig. 7. Pressure and temperature dependence of the relative volume V/V_0 for $LuFe_4P_{12}$. (V_0 is the equilibrium volume).

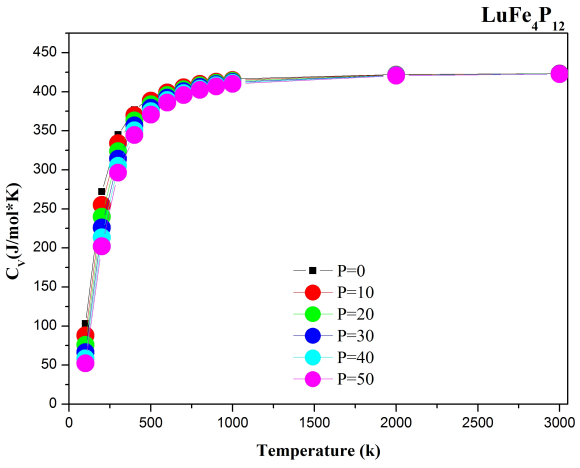

Fig. 9. The variation of the heat capacity C_v with temperature at different pressures for $LuFe_4P_{12}$.

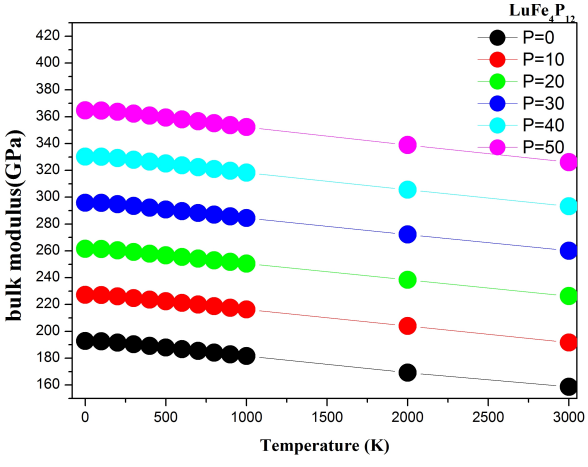

Fig. 8. The variation of the bulk modulus as a function of temperature at different pressures for $LuFe_4P_{12}$.

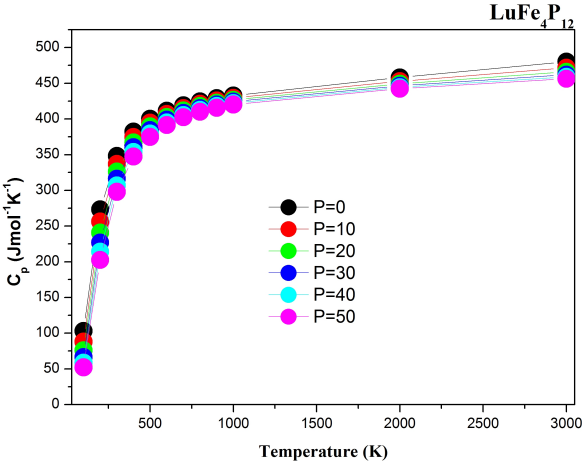

Fig. 10. The heat capacity at a constant pressure C_P versus temperature at different pressures for $LuFe_4P_{12}$.

$$\alpha = \frac{\gamma C_V}{B_T T} \tag{25}$$

$$\gamma = -\frac{d\ln\theta(V)}{d\ln V} \tag{26}$$

The thermal properties are determined in the temperature range of 0 to 3000 K in LDA calculation. The pressure effect is studied in 0 to 50 GPa range for $LuFe_4P_{12}$. The dependence of the primitive cell volume of temperature, using LDA, is shown in Fig. 7. The ratio V/V_0 decreases almost linearly with increasing temperature. For a given temperature, the primitive cell volume decreases as pressure increases. Fig. 8 shows the bulk modulus variation versus temperature at a given pressure. One can notice that the bulk modulus, a property of a material which defines its resistance to volume change when compressed, is nearly constant from 0 to 100 K and decreases linearly when increasing temperature from $T > 100$ K. The compressibility increases with temperature increase at a given pressure and decreases with pressure at a given

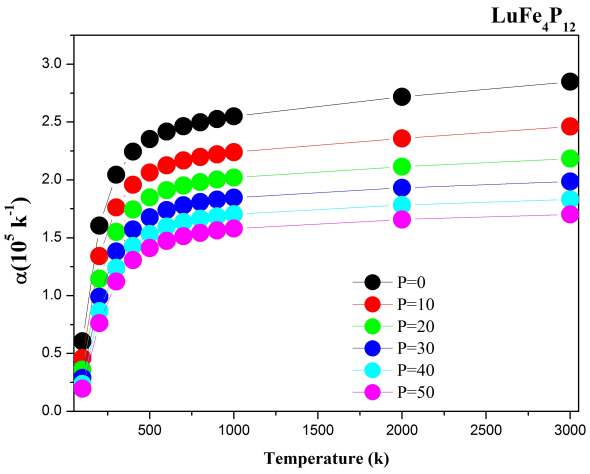

Fig. 11. The variation of the thermal expansion coefficient α as a function of temperature at different pressures for $LuFe_4P_{12}$.

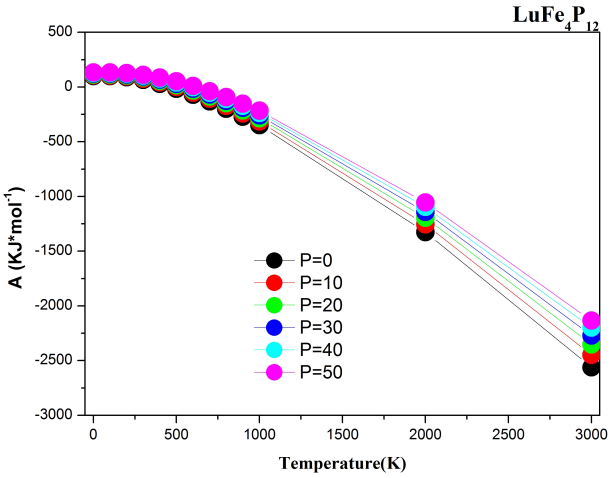

Fig. 13. The variation of Helmholtz free energy A as a function of temperature at different pressures for $LuFe_4P_{12}$.

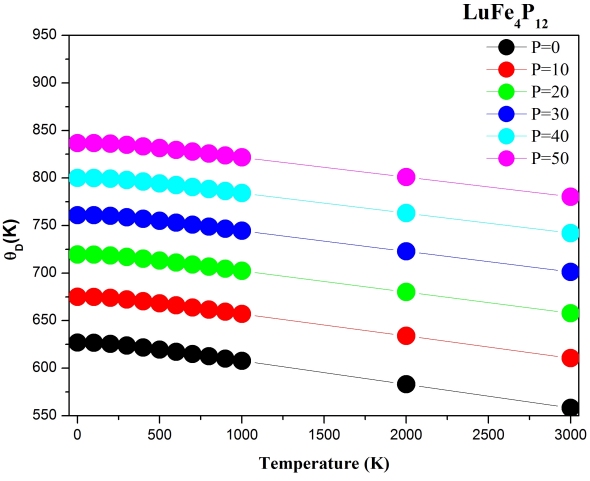

Fig. 12. The variation of the Debye temperature as a function of temperature at different pressures for $LuFe_4P_{12}$.

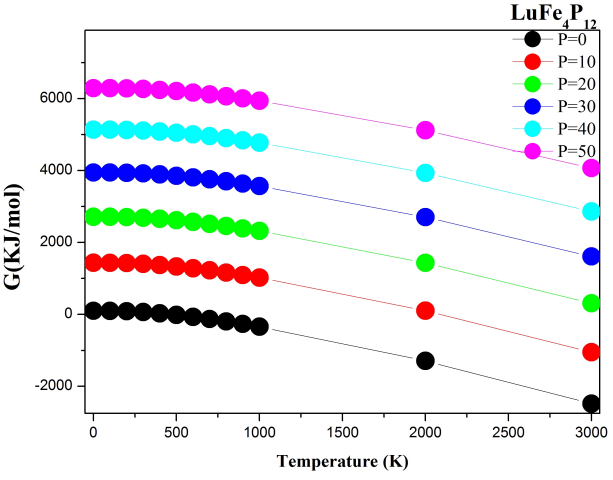

Fig. 14. Gibbs energy calculated as a function of temperature at different pressures for $LuFe_4P_{12}$.

temperature. These results show that the effect of increased pressure on the material is the same as that of temperature. At 300 K and zero pressure, the bulk modulus for our compound is 190.4 GPa. The variation of the heat capacities C_V versus temperature at 0, 10, 20, 30, 40 and 50 GPa pressures is shown in Fig. 9. It is shown that with increasing temperature, C_V values increase rapidly at a lower temperature, then they increase slowly at the high temperature and tend to the Petit and Dulong limit [39], which is common to all solids at high temperature. Thus, when $T < 1000$ K, the heat capacity C_V depends on both temperature and pressure effects. When the temperature is constant, the C_V decreases with the applied pressures; C_V tends to approach 422.61 $(J \cdot mol^{-1} \cdot K^{-1})$. The variation of the heat capacity C_P with pressure and temperature in the ranges of 0 to 50 GPa and 0 to 3000 K is shown in Fig. 10. With increasing temperature, the variation of C_P values at lower temperature is similar to that of C_V. However, in the high-temperature-range, the change tendency of C_P exhibits apparently different features under

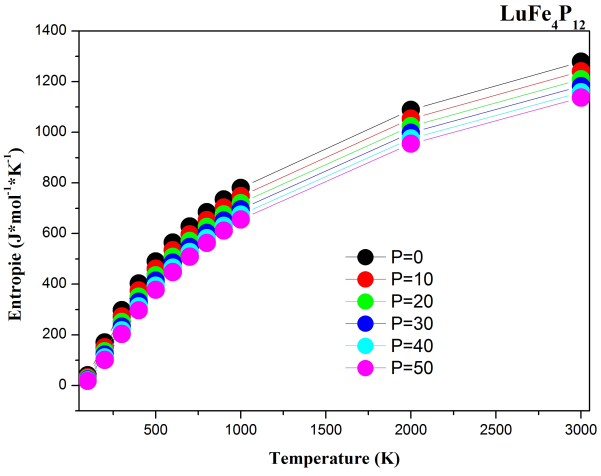

Fig. 15. The variation of the entropy (S) as a function of temperature at different pressures for $LuFe_4P_{12}$.

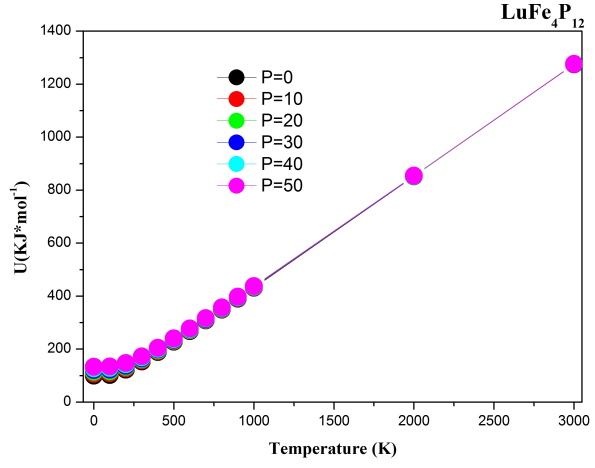

Fig. 16. The variation of the internal energy as a function of temperature at different pressures for $LuFe_4P_{12}$.

different pressures. C_P values decrease with increasing pressures and do not converge to a constant value. The C_P increases at higher temperature. Fig. 11 shows the variation of volume expansion coefficient α as a function of temperature and pressure, using LDA. It is shown that at a given pressure, α increases sharply with increasing of temperature up to 500 K. When T $>$ 500 K, α starts increasing gradually with temperature and the tendency of the increment becomes very moderate, which means that the temperature dependence of α is very small at high temperature. For a given temperature, α decreases dramatically with increasing of pressure. Using LDA, α increases sharply with the increase of temperature up to 200 K. Above this temperature, α tends gradually to a linear increase with temperature. However, the increment becomes moderate, which means that the temperature dependence of α is very small at high temperature. At 300 K and zero pressure, the value of volume expansion coefficient α is 2.04466×10^{-5} K^{-1}. Fig. 12 displays the dependence of Debye temperature θ_D on temperature and pressure. It can be seen that θ_D is nearly constant from 0 to 200 K and decreases linearly with increasing of temperature from T $>$ 200 K. It is also shown that when the temperature is constant, the Debye temperature increases almost linearly with applied pressure. Our calculated θ_D at zero pressure and 300 K temperature equals to 623.78 K. This might be an indication that the quasi-harmonic Debye model is a very reasonable alternative to account for the thermal effects at a low cost in terms of computational time. The pressure dependence of Helmholtz free energy A for $LuFe_4P_{12}$ at different temperatures is depicted in Fig. 13; the free energy A decreases gradually with increasing of temperature at a given pressure and decreases with pressure at a given temperature. Fig. 14 displays the dependence of the Gibbs free energy G on temperature and pressure. It can be seen that the Gibbs free energy G is nearly constant from 0 to 100 K and decreases linearly with increasing of temperature from T $>$100 K. It is also shown that when the temperature is constant, the Gibbs free energy G increases almost linearly with the applied pressure. The pressure-dependence of entropy for $LuFe_4P_{12}$ under different temperatures is depicted in Fig. 15. The entropies decrease with pressure and increase with temperature. Obviously, the entropy is more sensitive to the temperature than the pressure. The calculated internal energy for $LuFe_4P_{12}$ as a function of pressure for different temperatures is depicted in Fig. 16. It can be seen that the total internal energy increases with pressure and temperature. It is more sensitive to the temperature than the pressure.

4. Conclusions

In this work, we have studied the structural, elastic, electronic and thermodynamic properties of the filled skutterudite $LuFe_4P_{12}$ using the FP-LMTO method within the LDA calculations. The calculated lattice constants are in good agreement with the other available data. The computed spin-polarized band structure for $LuFe_4P_{12}$ exhibits metallic character. The elastic constants C_{ij}, bulk modulus B, shear modulus G, Young's modulus E and Poisson's ratio ν of $LuFe_4P_{12}$ compound have been calculated versus hydrostatic pressure up to 50 GPa using LDA calculation. The calculated Poisson ratio ν of $LuFe_4P_{12}$ at various pressures is around 0.3. This indicates that this compound is highly ionic. The obtained values of the Young's modulus of our compound is higher than 90 GPa; thus, this material will show large stiffness By analyzing the B/G ratio, we conclude that $LuFe_4P_{12}$ can be classified as a ductile material. The anisotropy factor suggests that $LuFe_4P_{12}$ compound exhibits anisotropic elasticity. Furthermore, we have estimated the sound velocities (v_l, v_t and v_m) and the Debye temperature for $LuFe_4P_{12}$ with pressure in the ranges of 0 to 50 GPa. Through the quasi-harmonic Debye model, the dependence of the primitive cell volume, expansion coefficient α, bulk modulus, heat capacity, Debye temperature θ_D, Helmholtz free energy A, Gibbs free energy G, entropy S and internal energy U on temperature and pressure have been obtained successfully.

Acknowledgements

Y.A. would like to acknowlegde the University Malaysia Perlis for Grant No. 9007-00111 and the TWAS-Italy for the full support of his visit to the JUST-Jordan under the TWAS-UNESCO Associateship.

References

[1] SALES B.C., GSCHNEIDNERJR K.A., BUNZLI J.C.G., PECHARSKY V.K., *Handbook on the Physics and Chemistry of Rare Earths*, Elsevier, Amsterdam, 2003, p. 211.

[2] BRAUN D.J., JEITSCHKO W., *J. Less Common Met.*, 72 (1980), 147.

[3] BAUERE D., BERGER S.T., GALATANU A., MICHOR H., PAUL CH., HILSCHER G., TRAN V.H., GRYTSIV A., ROGLL P., *Materials*, 226 (2001), 674.

[4] MEISNER G.P., STEWART G.R., TORIKACHVILI M.S., MAPLE M.B., in: ECKERN U., SCHMID A., WEBER W., WUHL H. (Eds.), *Proceedings of the 17th International Conference on Low Temperature Physics*, Elsevier, Amsterdam, 1984, p. 711.

[5] SHIROTANI I., UCHIUMI T., OHNO K., SEKINE C., NAKAZAWA Y., KADONA K., TODO S., YAGI T., *Phys. Rev. B*, 56 (1997), 7866.

[6] TORIKACHVILI M.S., ROSSEL C., MCELFRESH M.W., MAPLE M.B., GUERTIN R.P., MRISNER G.P., *J. Magn. Magn. Mater.*, 54 (1986), 365.

[7] DANEBROCK M.E., EVERS C.B.H., JEITSCHKO W., *J. Phys. Chem. Solids*, 57 (1996), 381.

[8] BAUER E.D., SLEBARSKI A., FREEMAN E.J., SIIRVENT C., MAPLE M.B., *J. Phys.-Condens. Mat*, 13 (2001), 4495.

[9] TAKEDA N., ISHIKAWA M., *J. Phys.-Condens. Mat.*, 13 (2001), 5971.

[10] SHIROTANI I., UCHIUMI T., OHNO K., SEKINE C., NAKAZAWA Y., KANODA K., TODO S., YAGI T., *Phys. Rev. B*, 56 (1997), 7866.

[11] BAUERE D., FREDERICK N.A., HO P.-C., ZAPF V.S., MAPLE M.B., *Phys. Rev. B*, 65 (2002), 100506.

[12] SHIROTANI I., UCHIUMI T., SEKINE C., HORI M., KIMURA S., HAMAYA N., *J. Solid State Chem.*, 142 (1999), 146.

[13] NAKOTTE H., DILLEY N.R., TORIKACHVILI M.S., BORDALLO H.N., MAPLE M.B., CHANG S., CHRISTIANSON A., SCHULTZ A.J., MAJKRZAK C.F., SHIRANE G., *Physica B*, 280 (1999), 259.

[14] ICHIMIN S., YOUSUKE S., KUNIHIRO K., CHIHIRO S., TAKEHIKO Y., *J. Solid State Chem.*,174 (2003), 32.

[15] SAVRASOV S., SAVRASOV D., *Phys. Rev. B*, 46 (1992), 12181.

[16] SAVRASOV S.Y., *Phys. Rev. B*, 54 (1996), 16470.

[17] `http://physics.njit.edu/savrasov`.

[18] PERDEW J.P., *Phys. Rev. B*, 33 (1986), 8822.

[19] PERDEW J.P., WANG Y., *Phys. Rev. B*, 45 (1992), 13244.

[20] BLOCHL P.E., JEPSEN O., ANDERSEN O.K., *Phys. Rev. B*, 49 (1994), 16223.

[21] MURNAGHAN F.D., *P. Natl. Acad. Sci. USA*, 30 (1944), 244.

[22] MEHL M.J., KLEIN B.K., PAPACONSTANTOPOULOS D.A., *Intermetallic compounds: principle and practice*, in: WESTBROOK J.H., FLEISCHEIR R.L. (Eds.), *Principles*, John Wiley & Sons, 1995.

[23] VOIGT W., *Lehrbush der Kristallphysik*, Taubner, Leipzig, (1928).

[24] SCHREIBER E., ANDERSON O.L., SOGA N., *Elastic Constants and Their Measurements*, McGraw-Hill, New York, 1973.

[25] BORN M., *Math. Proc. Cambridge*, 36 (1940), 160.

[26] BORN M., HUANG K., *Dynamical Theory of Crystal Lattices*, Oxford University Press, London, 1956.

[27] TVERGAARD V., HUTCHINSON J.W., *J. Am. Ceram. Soc.*, 71 (1988), 157.

[28] PUGH S.F., *Philos. Mag.*, 45 (1954), 823.
[29] WACHTER P., FILZMOSER M., REBIANT J., *Physica B*, 293 (2001), 199.
[30] VOIGT W., *Lehrbuch der Kristallphysik*, Taubner, Leipzing, 1929.
[31] SCHREIBER E., ANDERSON O.L., SOGA N., *Elastic constants and their measurements*, Mc Graw-Hill, New York, 1973.
[32] BLANCO M.A., FRANCISCO E., LUANA V., *Comput. Phys. Commun.*, 158 (2004), 57.
[33] PETIT A.T., DULONG P.L., *Ann. Chim. Phys.*, 10 (1819), 395.
[34] AMERI M., ABDELMOUNAIM B., SEBANE M., KHENATA R., VARSHNEY D., BOUHAFS B., AMERI I., *Mol. Simulat.*, 40 (15) (2014), 1236.
[35] AMERI M., SLAMANI A., ABIDRI B., AMERI I., ALDOURI Y. , BOUHAFS B., VARSHNEY D., ADJADJ A., LOUAHALA N., *Mat. Sci. Semicon. Proc.*, 27 (2014), 379.
[36] MEISNER G.P., TORIKACHVILI M.S., YANG K. N., MAPLE M.B., GUERTIN R.P., *J. Appl. Phys.*, 57 (1985), 3073.
[37] JEITSCHKO W., BRAUN D.J., *Acta Crystallogr. B*, 33 (1977), 3401.
[38] ACKERMAN J.F., WOLD A., *J. Phys. Chem Solids*, 38 (1977), 1013.
[39] FRANCISCO E., RECIO J.M., BLANCO M.A., MARTIN PENDAS A., COSTALES A., *J. Phys. Chem.*, 102 (1998), 1595.
[40] BLANCO M.A., PENDAS M.A., FRANCISCO E., RECIO J.M., FRANCO R., *J. Mol. Struct.*, 368 (1996), 245.
[41] FRANCISCO E., BLANCO M.A., SANJURJO G., *Phys. Rev. B*, 63 (2001), 094107.
[42] SHIROTANI I., SHIMAYA Y., KIHOU K., SEKINE C., YAGIB T., *J. Solid State Chem.*, 174 (32 – 34) (2003), 1013.

Received 2015-03-15
Accepted 2015-09-04